

The Northernmost CAMP: $^{40}\text{Ar}/^{39}\text{Ar}$ age, Petrology and Sr-Nd-Pb Isotope Geochemistry of the Kerforne Dike, Brittany, France

Fred Jourdan¹, Andrea Marzoli¹, Herve Bertrand², Michael Cosca³, Denis Fontignie¹

The Central Atlantic Magmatic Province (CAMP) is defined by tholeiitic basaltic flows and dikes associated with the initial break-up of Pangea at 200 Ma, preceding the opening of the Atlantic Ocean. These tholeiites occur in once-contiguous parts of North America, Africa, South America and Europe over a total area of about 7 million square kilometers. The Kerforne dike, located in Brittany (NW France), represents the northernmost outcrop of this province. Due to its orientation and location, more than 1500 Km from the Early Jurassic Atlantic rift, like other CAMP dikes, it can not be considered as the magmatic expression of the Central Atlantic rifting. Despite its distal position, this dike has an Ar/Ar age (193 ± 3 Ma, obtained on plagioclase separates) similar to the CAMP tholeiites. Kerforne dolerites are characterized by augite and minor plagioclase phenocrysts. According to petrographic observation and microprobe analyses, some of these plagioclases contain resorbed high-An (An_{85}) possibly xenocrystic cores which may be evidence of interaction with a mafic lower crust. The low- TiO_2 (1.0 wt%) tholeiitic Kerforne basalts are characterized by negative Nb anomalies, by a positive correlation between ϵ_{Sr} and ϵ_{Nd} , by high radiogenic $^{207}\text{Pb}/^{204}\text{Pb}$ in comparison to relatively unradiogenic $^{206}\text{Pb}/^{204}\text{Pb}$, and by an enrichment in LREE relative to HREE. These chemical features, along with the mineralogic observations, are indicative of a minor contamination with mafic lower crust, like that represented by granulitic xenoliths of the Massif Central, France. By contrast, contamination with the silicic upper crust (e.g., with the granitic basement) was negligible. The isotopic compositions of the little contaminated Kerforne basalts are similar to those of most other CAMP low- TiO_2 basalts, and are different from those of most oceanic basalts. It is suggested that this high $^{87}\text{Sr}/^{86}\text{Sr}$ and $^{207}\text{Pb}/^{204}\text{Pb}$ isotopic signature was inherited by interaction of primitive mantle with metasomatized portions of the continental lithospheric mantle, similar to the sources of Variscan lamproites of Brittany. Moreover, The contribution of an OIB mantle component may be ruled out as the Kerforne mantle source was isotopically different from those of the oceanic islands which have been suggested to represent the present-day expression of the hypothetical CAMP mantle plume.

¹ Section de Sciences de la Terre; Université de Genève, Switzerland

² Ecole Normale Supérieure et UCBL, Laboratoire des Sciences de la Terre,

³ Institute of Mineralogy and Geochemistry, University of Lausanne, Switzerland

1. INTRODUCTION

At about 200 Ma, before the opening of the Central Atlantic and the breakup of Pangea vast volumes of continental tholeiitic basaltic magmas were emplaced over an area of at least 7 million square kilometers in South and North America, Western Africa and Southwestern Europe [e.g., *Bertrand*, 1991; *Deckart et al.*, 1997; *Marzoli et al.*, 1999; *McHone*, 2000; *Hames et al.*, 2000]. The Central Atlantic Magmatic Province (CAMP) is mainly represented by intrusions (dikes and sills) and minor erosional remnants of lava flows. Like most basalts of other large continental igneous provinces, including continental flood basalts (CFB), the CAMP basalts are subdivided into two geochemical subgroups, low- and high-Ti, respectively. The vast majority of CAMP basalts are low-TiO₂ (< 2.0 wt%) tholeiites characterized by a lithospheric (crust and/or mantle) isotopic signature. The only known high-TiO₂ CAMP tholeiites occur in the once contiguous Equatorial regions of Africa (Liberia) and South America [N-E Brazil and Guyana; *Dupuy et al.*, 1988; *Bertrand et al.*, 1999; *De Min et al.*, present volume].

The northernmost occurrence of the CAMP is represented by the Kerforne dike of Western Brittany, France. It is part of the European subprovince of the CAMP, which includes the lava flows, sills and dikes of the Pyrenees and of the Iberian peninsula [*Alibert*, 1985; *Bertrand et al.*, 1987; *Beziat et al.*, 1991; *Sebai et al.*, 1991; *Demant et al.*, 1996; Fig. 1]. We present here the first integrated petrographic, mineralogic, geochemical, isotopic and Ar/Ar geochronological study of a CAMP dike. The present study is also an attempt to understand the petrogenesis of basalts of the CAMP, within the context of a relatively well studied region such as Brittany and France in general.

2. GEOLOGICAL SETTING AND SAMPLING

The Kerforne dike is located in Brittany in northwestern France (Fig. 1). The tholeiitic magma intruded a rejuvenated SE-NW oriented Hercynian fault system. By the time of magmatic intrusion, during the earliest Jurassic (see below), the Kerforne dike was situated at the western end of an extensional basin. This ranged from Catalonia to the Basque Countries, before the opening of the Gulf of Biscay, which occurred in the Cretaceous [*Moreau et al.*, 1997]. The orientation of this basin was orthogonal to the principal Central Atlantic and Alpine Tethys rifts [Fig. 1a; *Stampfli et al.*, 1998], and roughly parallel to the

Kerforne dike. Located at about 1500 km from the main Central Atlantic and Tethys rifts, the dike was aligned with the tholeiitic magmatic rocks of the Pyrenees [*Beziat et al.*, 1991], located 600 km to the south-west (Fig. 1a).

The comparable paleopole for Kerforne [*Sichler and Perrin*, 1993] and other CAMP basalts is indicative of a similar age. This is consistent with K/Ar dates obtained on whole rock, biotite and plagioclase of the Kerforne dike, despite the wide range displayed by these ages, from 170 to 210 Ma [*Caroff et al.*, 1995].

The dike intrudes igneous and metamorphic rocks of the Armorican massif, which was part of the Variscan arc [e.g., *Matte*, 1986]. Two major roughly E-W oriented faults, the North and South Armorican Shear Zones, separate three major units in western Brittany. The dike intrudes the central and southern structural units, and terminates near the intersection between the North Armorican Shear Zone and the Atlantic ocean. The Central Armorican domain consists mainly of low grade meta-sedimentary rocks, whose protoliths vary in age from Cambrian to Carboniferous. Minor volcanic rocks (lamproites, tholeiitic basalts and silicic flows) and granites intruding along the South Armorican Shear Zone were emplaced during the Variscan orogeny [*Turpin et al.*, 1988; *Caroff et al.*, 1996; *Bernard-Griffiths et al.*, 1985]. The South Armorican domain is a high grade metamorphic belt, built up of gneiss, schist and granite of Ordovician to Carboniferous age [*Bernard-Griffiths et al.*, 1985].

The 100 km long Kerforne dike has a thickness of several meters, up to a maximum of 30 m at the Brenterc'h North and Pors Milin outcrops. In all outcrops, the sub-vertical (75°) to vertical dike follows a 110-130°N orientation and generally crosscuts the foliation of the basement rocks. A complete description of the outcrops of Kerforne basalts is provided by *Caroff et al.* [1995]. For this study, only the most representative and best preserved sites within the Central Armorican domain have been sampled (Fig. 1b), which, from SE to NW are:

- 1) The 10 m thick dike close to Douarnenez (samples B1 and B2; Table 1) which intrudes a slightly metamorphosed trondhjemitic rock of Early Permian age (sample B3, 281 ± 5 Ma, ⁴⁰Ar/³⁹Ar plateau age; see below; Table 1). Leucogranites cropping out a few kilometers to the South, still within the Central Armorican domain, have been dated (Rb/Sr) at 344 ± 7 Ma [*Bernard-Griffiths et al.*, 1985].

- 2) The slightly altered dike at Camaret, on the Crozon peninsula (B4 and B5), which is about 10 m thick. Its country rocks are Carboniferous meta-sedimentary units, weakly folded during the Hercynian orogeny.

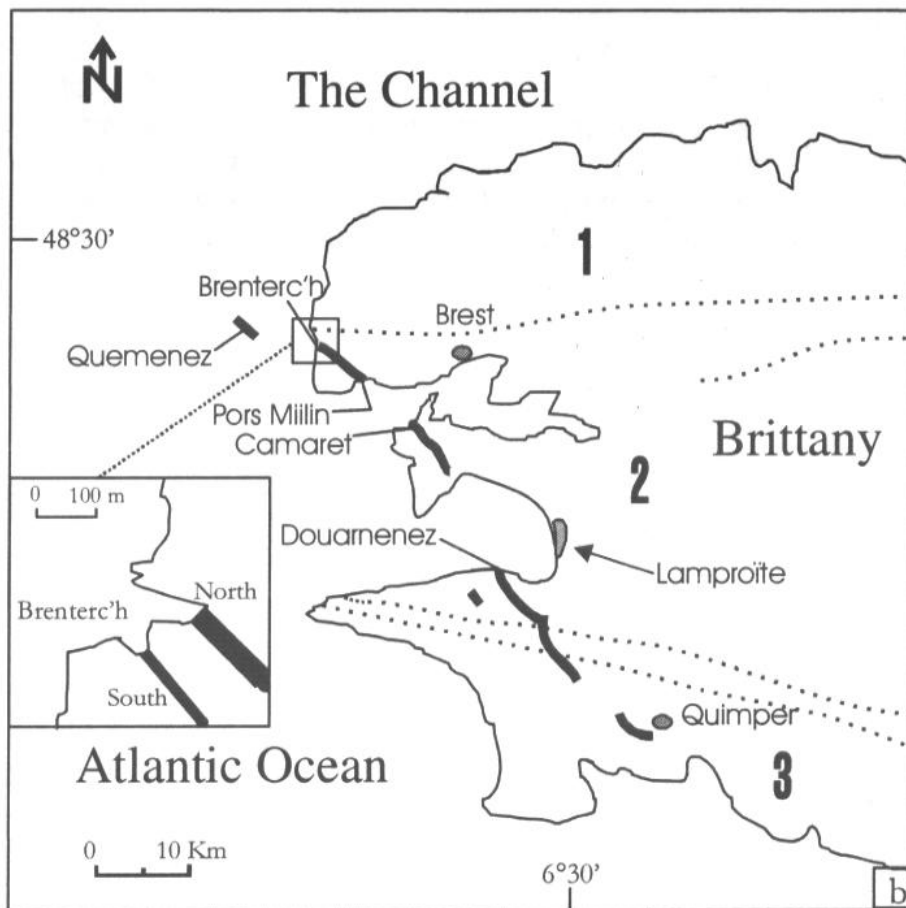
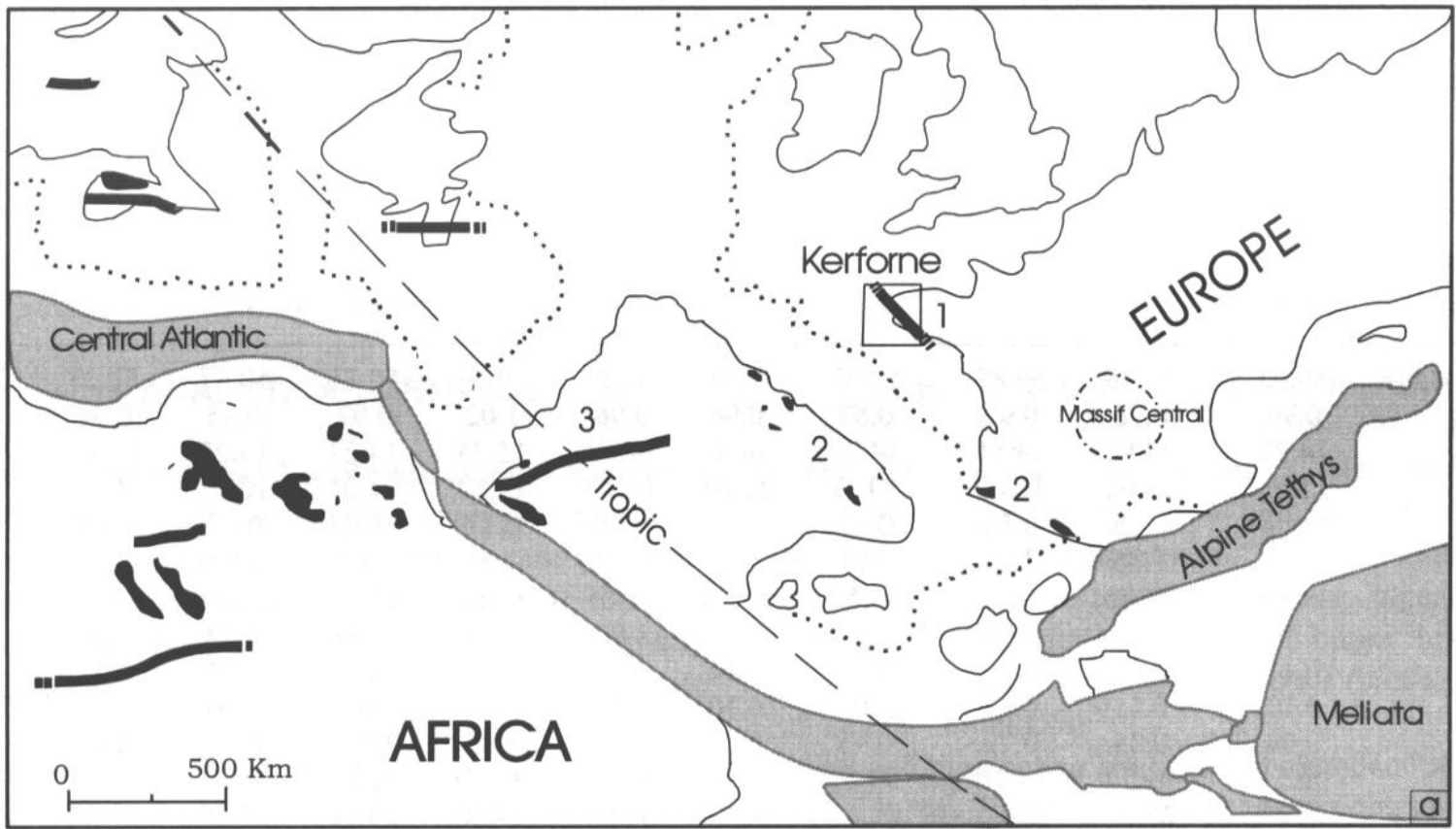


Figure 1. a: Location map of the European and North African CAMP [Bertrand, 1991; Sebai *et al.*, 1991; McHone, 2000] in an Early Jurassic Pangea reconstruction adapted from Stampfli *et al.* [1998]. Dikes are represented by bold line, magmatic flows by dark areas and continental margins by dotted lines; solid lines represent the present continental shape. 1: Kerforne dike; 2: Pyrenean sills; 3: Messejana dike.

(b): Sketch map of western Brittany showing sample locations of the Kerforne dike. The dike is represented by a bold discontinuous line and the North and South Armorican shear zones by dotted lines, separating the North (1), Central (2) and South (3) Armorican zones. Note location of lamproitic rocks [Turpin *et al.*, 1988]. Inset represents sketch map of Brenterc'h outcrops.

Table 1. Major (wt%), trace and REE (ppm) compositions, and CIPW-normative quartz and olivine of selected Kerforne dike samples plus one wall-rock sample. [$Mg\# = 100 * Mg / (Mg + Fe^{2+})$; $Fe_2O_3/FeO = 0.17$], as calculated for QFM buffered fO_2 , at 1 kbar, by using MELTS; *Ghiorso and Sack* [1995].

| Sample | Kerforne basalts | | | | | | | | | | granite |
|--------------------------------|------------------|-------|-------|-------|-------|-------|--------|-------|-------|-------|---------|
| | B1 | B 2 | B 4 | B 5 | B 7 | B 8 | B 9 | B 11 | B 12 | B 13 | B3 |
| SiO ₂ (wt.%) | 50.08 | 50.25 | 50.89 | 50.42 | 49.90 | 50.29 | 49.50 | 50.71 | 50.47 | 51.23 | 72.21 |
| TiO ₂ | 0.96 | 0.98 | 0.97 | 0.87 | 0.94 | 0.96 | 1.02 | 0.97 | 0.95 | 0.94 | 0.25 |
| Al ₂ O ₃ | 14.22 | 14.80 | 14.51 | 14.72 | 14.52 | 14.60 | 15.35 | 14.27 | 14.25 | 13.97 | 13.95 |
| Fe ₂ O ₃ | 11.03 | 11.02 | 10.69 | 10.39 | 11.03 | 11.19 | 11.59 | 11.04 | 10.87 | 10.77 | 2.83 |
| MnO | 0.19 | 0.18 | 0.16 | 0.16 | 0.17 | 0.18 | 0.17 | 0.17 | 0.17 | 0.17 | 0.04 |
| MgO | 7.93 | 7.86 | 7.47 | 7.81 | 8.15 | 8.04 | 7.31 | 7.62 | 7.71 | 7.71 | 0.80 |
| CaO | 11.66 | 11.72 | 11.55 | 11.52 | 11.34 | 11.75 | 10.85 | 11.52 | 11.71 | 11.67 | 1.88 |
| Na ₂ O | 1.90 | 2.02 | 1.94 | 1.90 | 2.00 | 1.95 | 2.04 | 2.00 | 1.92 | 1.96 | 3.30 |
| K ₂ O | 0.41 | 0.43 | 0.56 | 0.79 | 0.81 | 0.52 | 0.38 | 0.65 | 0.34 | 0.57 | 2.75 |
| P ₂ O ₅ | 0.10 | 0.11 | 0.11 | 0.09 | 0.10 | 0.10 | 0.12 | 0.11 | 0.10 | 0.10 | 0.10 |
| LOI | 0.99 | 0.35 | 0.79 | 0.95 | 0.61 | 0.23 | 1.82 | 0.56 | 0.77 | 0.45 | 1.19 |
| Sum | 99.51 | 99.77 | 99.70 | 99.68 | 99.62 | 99.86 | 100.21 | 99.67 | 99.30 | 99.57 | 99.29 |
| Mg# | 60.70 | 60.51 | 60.01 | 61.77 | 61.34 | 60.68 | 57.56 | 59.72 | 60.38 | 60.58 | 37.82 |
| Nb (ppm) | 5 | 5.5 | 5 | 5 | 5 | 5.3 | 5 | 5.4 | 5 | 5.3 | 3 |
| Zr | 74 | 81 | 75 | 75 | 69 | 78 | 78 | 80 | 74 | 78 | 191 |
| Y | 20 | 20 | 21 | 17.3 | 19 | 21 | 22 | 22 | 19 | 21 | 34 |
| Sr | 162 | 163 | 179 | 184 | 177 | 167 | 168 | 167 | 161 | 186 | 94 |
| Rb | 16 | 12.7 | 18 | 18.7 | 25 | 15.4 | 16 | 17.7 | 15 | 15.5 | 62 |
| Ni | 107 | 120 | 106 | 108 | 107 | 110 | 121 | 107 | 110 | 120 | 2 |
| Cr | 185 | 241 | 146 | 256 | 182 | 254 | 182 | 250 | 171 | 262 | 10 |
| V | 275 | 272 | 278 | 252 | 271 | 259 | 304 | 271 | 273 | 267 | 24 |
| Ba | 93 | 124 | 132 | 149 | 102 | 133 | 63 | 108 | 82 | 118 | 258 |
| Sc | 26 | 25 | 23 | 23 | 27 | 34 | 34 | 26 | 26 | 22 | 5 |
| U | - | 0.4 | 0.3 | - | - | 0.3 | 0.4 | 0.4 | - | 0.3 | 3 |
| Th | - | 1.2 | 1.2 | - | - | 1.2 | 1.3 | 1.2 | - | 1.2 | - |
| Pb | - | 2 | - | 3 | - | 4 | 3 | 2 | - | 2 | - |
| La | - | 7.4 | 7.6 | - | - | 7.6 | 8.4 | 7.9 | - | 7.5 | - |
| Ce | - | 17.6 | 17.7 | - | - | 17.9 | 19.8 | 18.8 | - | 17.7 | - |
| Pr | - | 1.9 | 1.9 | - | - | 1.9 | 2.1 | 2.0 | - | 1.9 | - |
| Nd | - | 10.3 | 10.7 | - | - | 10.4 | 11.5 | 10.9 | - | 10.4 | - |
| Sm | - | 2.9 | 2.9 | - | - | 2.9 | 3.2 | 3.0 | - | 2.8 | - |
| Eu | - | 0.92 | 0.94 | - | - | 0.96 | 1.06 | 0.94 | - | 0.9 | - |
| Gd | - | 3.0 | 3.3 | - | - | 3.2 | 3.7 | 3.4 | - | 3.3 | - |
| Tb | - | 0.6 | 0.6 | - | - | 0.6 | 0.6 | 0.6 | - | 0.6 | - |
| Dy | - | 3.5 | 3.5 | - | - | 3.5 | 3.7 | 3.6 | - | 3.4 | - |
| Ho | - | 0.76 | 0.75 | - | - | 0.74 | 0.81 | 0.78 | - | 0.73 | - |
| Er | - | 2.2 | 2.2 | - | - | 2.2 | 2.4 | 2.3 | - | 2.3 | - |
| Tm | - | 0.3 | 0.3 | - | - | 0.3 | 0.3 | 0.3 | - | 0.3 | - |
| Yb | - | 2.1 | 2.1 | - | - | 2.0 | 2.2 | 2.2 | - | 2.1 | - |
| Lu | - | 0.31 | 0.31 | - | - | 0.32 | 0.32 | 0.33 | - | 0.32 | - |
| CIPW norm | | | | | | | | | | | |
| Quartz | 1.04 | 0.29 | 0.87 | 0.51 | - | 0.06 | 0.75 | 1.03 | 1.94 | 2.02 | - |
| Olivine | - | - | - | - | 2.98 | - | - | - | - | - | - |

3) The dike close to Pors Milin (B12 and B13), about 30 m thick, which is weakly altered on its northern side, and intrudes the Brest orthogneiss.

4) The northern (B7, B8, B9) and southern (B10 and B11) branches of the dike at Brenterc'h, which reach a thickness of 30 m and 15 m, respectively. These two branches of the dike are separated by 100 m and both intrude the Ploumouguet basement gneiss.

3. ANALYTICAL METHODS

A set of 10 basalts and 2 wall-rock granites have been selected for major and trace element analyses which have been performed at the University of Lausanne (Switzerland), by X-ray fluorescence (XRF), following methods described in Rhodes [1988], and with average analytical uncertainties of 1% for major elements, and 5% for trace elements. REE, Th and U (uncertainties < 3%) were measured on 6 samples at XRAL laboratories, Toronto, Canada, by VG Plasma-Quad inductively coupled plasma-mass spectrometer (ICP-MS), using Na₂O₂ fusion. Mineral analyses were made at the University of Lausanne, with a CAMECA SX50 electron microprobe, using 15 kV accelerating voltage, and 15 to 30 nA current during analyses of plagioclase and mafic minerals, respectively.

For Pb-Sr-Nd isotope analyses at the University of Geneva, Switzerland, 500 mg of hand-picked grains of six basalts and one granite sample were leached (HCl) before dissolution with HF+HNO₃ and HCl, and followed by standard element separation with chromatographic ion-exchange columns. Measurements were performed with a 7-collector Finnigan MAT 262 thermal ionization mass spectrometer. ⁸⁷Sr/⁸⁶Sr ratios were measured in semi-dynamic mode and are mass-fractionation corrected to a ⁸⁸Sr/⁸⁶Sr ratio of 8.375209. Measurement of standard E & A yielded an average value of 0.708028 ± 5 (2σ), n = 52. ¹⁴³Nd/¹⁴⁴Nd analyses were performed in semi-dynamic mode with ¹⁴⁶Nd/¹⁴⁴Nd mass fraction corrected to 0.721903. La Jolla Nd standard gave a value of 0.511832 ± 6 (2σ), n = 28. Pb isotopic compositions were measured in dynamic mode. SRM NBS 981 standard yielded values of 0.92 ± 0.05 (2σ), n = 132 and Pb concentration were determined by XRF.

Three hand picked plagioclase separates (about 30 mg of 100-200 μm crystals) of the dike (B2, B8 and B11) and one biotite separate of the granitic basement (B3) were selected for ⁴⁰Ar/³⁹Ar dating. Samples were irradiated for 12 hours in the Triga reactor at Oregon State University, USA, along with Fish Canyon sanidine (FCs)

neutron fluence monitors, for which an age of 28.02 Ma is adopted [Renne *et al.*, 1998]. Incremental heating from 550 to 1600 °C (15 steps for the plagioclase, 20 for the biotite) in a resistance furnace and analyses on a MAP-215.5 mass spectrometer were performed at the University of Lausanne, Switzerland. Ages were calculated considering the ⁴⁰K decay constants of Steiger and Jäger [1977]

4. PETROGRAPHY AND MINERALOGY

The tholeiitic dolerites display a fine grained sub-ophitic to ophitic texture which becomes sub-hyaline at the dike's margins at Brenterc'h. The main minerals are augitic clinopyroxene (cpx), plagioclase, pigeonite, olivine, and Fe-Ti oxides (magnetite and minor ilmenite). A few samples contain secondary minerals (biotite, sericite, calcite and amphibole).

Cpx and plagioclase are the most abundant phenocryst phases in the Kerferne dolerites. Cpx consists of large optically homogeneous augite (30-40 vol. %; Wo₃₁₋₄₂ En₄₆₋₅₇ Fs₆₋₁₁) plus minor pigeonite (0-5 vol. %; Wo₁₃₋₁₄ En₆₁₋₆₂ Fs₂₄). Pigeonite is usually confined to the rim of augite and never occurs as isolated crystals. Augite is Cr₂O₃-rich (up to 0.8 wt%) and relatively Al₂O₃ poor (up to 3 wt%). Ca, Cr and Mg# [100*Mg/(Mg+Fe²⁺), considering Fe₂O₃/FeO = 0.17] decrease toward the crystal rims, consistently with cpx evolution trends in tholeiitic magmas. The augite-pigeonite equilibrium crystallization temperature [Lindsley, 1983] is estimated at between 1150-1050 °C. For a temperature of 1100 °C the calculated augite crystallization pressure is about 3.5 ± 2 kbars [Nimis, 1995], suggesting a shallow crystallization.

Olivine represents 5 to 10 % of the rock and it occurs mainly as relatively large (up to 3 mm) resorbed crystals or as inclusions within augite microphenocrysts. Olivine is rarely fresh and is frequently replaced by bowlingite and iddingsite. Fresh portions of olivine phenocrysts are generally homogeneous and forsterite (Fo) poor (Fo₇₀₋₇₁). This suggests that olivine composition is out of equilibrium with the relatively little evolved host rock (Mg# = 57.6-61.8).

Plagioclase represents about 40-50 vol. % of the bulk rock and consists of two main textural and compositional types: (a) microlites and (b) sparse relatively large, optically zoned plagioclase phenocrysts, sometimes occurring as crystal aggregates (Table 2). The microlites have labradorite-andesine composition (An₇₄₋₄₂), which is consistent with the moderately evolved whole-rock compositions [Ca# = 100*Ca/(Ca+Na) = 73-76]. By contrast,

Table 2. Representative compositions of plagioclase phenocrysts and groundmass (gm) microlites. Molar % albite (Ab), anorthite (An) and orthoclase (Or) are shown.

| Sample Location | B2 Plag3 core | B7 Plag1 core | B9 Plag1 core | B9 Plag1 rim | B9 Plag2 core | B12 Plag2 core | B2 Plgm microlite | B8 Plgm microlite | B11 Plgm microlite |
|--------------------------------|---------------|---------------|---------------|--------------|---------------|----------------|-------------------|-------------------|--------------------|
| SiO ₂ (wt%) | 47.28 | 46.41 | 46.20 | 56.02 | 46.37 | 46.82 | 49.10 | 53.48 | 49.92 |
| Al ₂ O ₃ | 32.81 | 33.58 | 33.30 | 27.68 | 33.66 | 33.63 | 31.35 | 28.12 | 31.37 |
| Fe ₂ O ₃ | 0.57 | 0.69 | 0.58 | 0.85 | 0.69 | 0.60 | 0.67 | 0.94 | 0.59 |
| MgO | 0.24 | 0.13 | 0.24 | 0.04 | 0.25 | 0.23 | 0.12 | 0.14 | 0.15 |
| CaO | 17.32 | 17.47 | 17.41 | 9.96 | 17.44 | 17.21 | 15.13 | 11.88 | 14.98 |
| BaO | 0.00 | 0.03 | 0.01 | 0.02 | 0.04 | 0.01 | 0.00 | 0.02 | 0.05 |
| Na ₂ O | 1.62 | 1.63 | 1.53 | 5.67 | 1.52 | 1.63 | 2.81 | 4.56 | 3.01 |
| K ₂ O | 0.05 | 0.04 | 0.03 | 0.39 | 0.05 | 0.05 | 0.09 | 0.20 | 0.08 |
| Sum | 99.89 | 99.99 | 99.31 | 100.62 | 100.01 | 100.17 | 99.28 | 99.35 | 100.16 |
| Ab (Mol%) | 14.45 | 14.39 | 13.71 | 49.59 | 13.55 | 14.61 | 25.02 | 40.52 | 26.55 |
| An | 85.27 | 85.30 | 86.09 | 48.13 | 86.08 | 85.07 | 74.43 | 58.30 | 72.97 |
| Or | 0.28 | 0.26 | 0.18 | 2.24 | 0.31 | 0.31 | 0.55 | 1.18 | 0.48 |

plagioclase phenocrysts consist of rounded and resorbed high-An cores (An₈₀₋₈₆), mantled by labradorite rims with compositions similar to those of the groundmass microlites.

Compositional profiles across ten plagioclase phenocrysts with An₈₀₋₈₆ core have been obtained (cf., Fig. 2). According to experimental data [Panjasawatwong *et al.*, 1995] at anhydrous conditions, calcic plagioclase (An₈₅) crystallizes from extremely calcic magmas (e.g., Ca# = 85), i.e. substantially more calcic than Kerforne basalts and even more calcic than primary basalts obtained in peridotite melting experiments [e.g., Hirose and Kushiro, 1993]. Alternatively, high-An plagioclase crystallizes from hydrous magma ($Kd_{(Ca/Na)} > 1$), but there is no evidence that the tholeiitic Kerforne basalts were particularly rich in H₂O. We suggest therefore that the rounded-resorbed high-An cores are in fact xenocrysts crystallized from a relatively H₂O rich, little evolved magma and subsequently inherited by the Kerforne basalts.

Further constraints on the crystallization of plagioclase in Kerforne tholeiites has been obtained from minor element profiles (Fig. 2). In plagioclase phenocrysts with high-An cores, MgO decreases from about 0.25-0.30 wt% in the cores to less than 0.10 wt% at the rims. By contrast, K₂O increases from less than 0.10 wt% to 0.40-0.60 wt%. The composition of the magma from which the plagioclase crystallized can be calculated assuming equilibrium crystallization at a temperature of 1200 °C and adopting the partition coefficients of Bindeman *et al.* [1998]. High-An plagioclase cores may have crystallized from magmas with high MgO (> 10 wt%) and relatively high K₂O (ca. 0.5-1.0 wt%). Such compositions are different from those of Kerforne basalts. Minor element

compositions support the conclusion that the high-An plagioclase cores are not likely crystallized from the Kerforne basalts at equilibrium conditions.

The K₂O content in the outermost 20% of the plagioclase volume increases up to 0.60 wt%, while MgO decreases to low values. Such an important increase of K₂O and decrease of MgO requires that the plagioclase phenocrysts rims crystallized from an evolved residual liquid (with about 2 wt% K₂O and 2 wt% MgO).

5. AR/AR GEOCHRONOLOGY

For three basaltic samples only (B2, B8 and B11) we could obtain quantities of plagioclase separate (30-36 mg) sufficient for Ar/Ar dating. In general, a thin alteration zone affects plagioclase rims and fractures, as confirmed by an XRD analysis of a plagioclase separate of sample B8, which contains a little amount of sericite (about 5 wt%). Most of the alteration could be eliminated for sample B2, which contains plagioclase phenocrysts (cf., Fig. 2), but not for the fine grained plagioclase of B8 and B11 (about 100 µm diameter).

The three dated basalts yielded plateau ages of 189.0 ± 3.0 Ma (B2), 177.0 ± 3.0 Ma (B11) and 173.0 ± 3.0 Ma (B8; all errors are given at the 2σ confidence level; Fig. 3; Table 3). Apparent age and Ca/K spectra of B2 and of the Brenterch's basalts (B8 and B11) are different. B2 displays plateau steps associated with high apparent Ca/K (generally >40), while Ca/K for plateau steps of B8 and B11 is generally low (<10). For B8 and B11, the oldest apparent ages are obtained for steps 5-6 (800-850 °C) which also have the highest apparent Ca/K (about 20), whereas subsequent plateau steps decrease in apparent

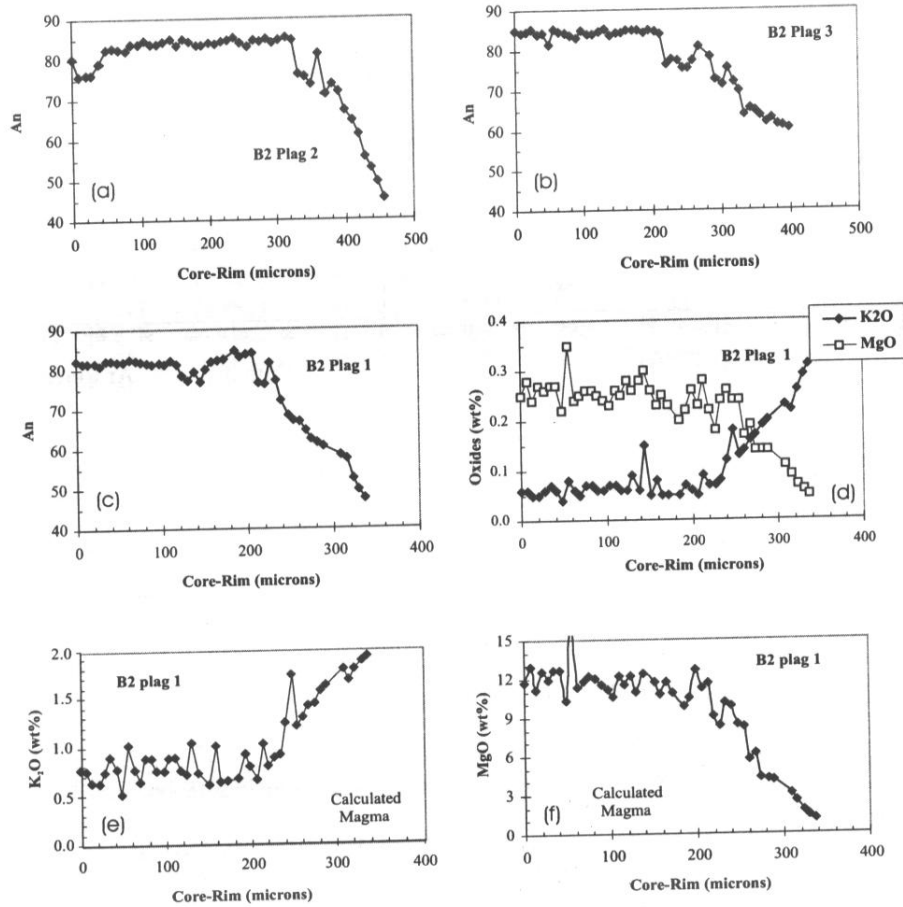


Figure 2. a-d: Representative plagioclase anorthite of B2 (An, molar %), K₂O and MgO (wt%) compositional profiles (Plagioclase 1, 2, and 3 of). Similar profiles were obtained for the analyzed plagioclase phenocrysts of B7, B9 and B12. e and f: calculated MgO and K₂O concentrations of magma in equilibrium with the analyzed plagioclase. Partition coefficients after *Bindeman et al.* [1998], assuming a temperature of 1200 °C.

age and Ca/K. In general, the absolute amount of released ⁴⁰Ar was substantially (up to 5 times) higher for B8 and B11 than for B2, suggesting that the two analyzed mineral separates of the Brenterc'h basalts were richer in potassium.

Isochron ages (MSWD = 0.48-1.33, 9-11 steps) of the three samples are slightly older than the plateau ages (193.4 ± 3.7 Ma, 178.0 ± 3.5 Ma, and 174.3 ± 3.3 Ma for B2, B11 and B8, respectively). The initial ⁴⁰Ar/³⁶Ar of the three samples is always lower than the atmospheric ratio (233-284), suggesting a depletion of ⁴⁰Ar* (i.e., an excess of ³⁹Ar/⁴⁰Ar).

In general, the analyzed mineral separates, particularly those of B8 and B11, seem to consist of partially altered (sericitized) plagioclase, as suggested by the apparent Ca/K which is substantially lower than that of plagioclase (>40; cf., Table 2). Even if the XRD analyses suggest

that sericite doesn't exceed a few wt% of the dated mineral separate, the different K₂O concentration of plagioclase (<0.50 wt%) and sericite (probably about 10 wt%) suggests that the obtained age refers to a hydrothermal event (sericite crystallization) and not to the magmatic age (plagioclase crystallization). Moreover, the fine-grained mineral separate of the Brenterc'h samples may have been affected by some ³⁹Ar recoil, as suggested by the decreasing apparent ages associated with decreasing Ca/K [cf. *Onstott et al.*, 1995]. Altogether, (post-magmatic) alteration and recoil result in apparent ages younger than the magmatic age.

Notably however, the dated sample (B2) displaying the highest measured Ca/K, yields the highest plateau and isochron ages. These ages of B2, and particularly its isochron age (193.4 ± 3.7 Ma) are probably the closest estimate of the magmatic age of the Kerforne dike, and fall

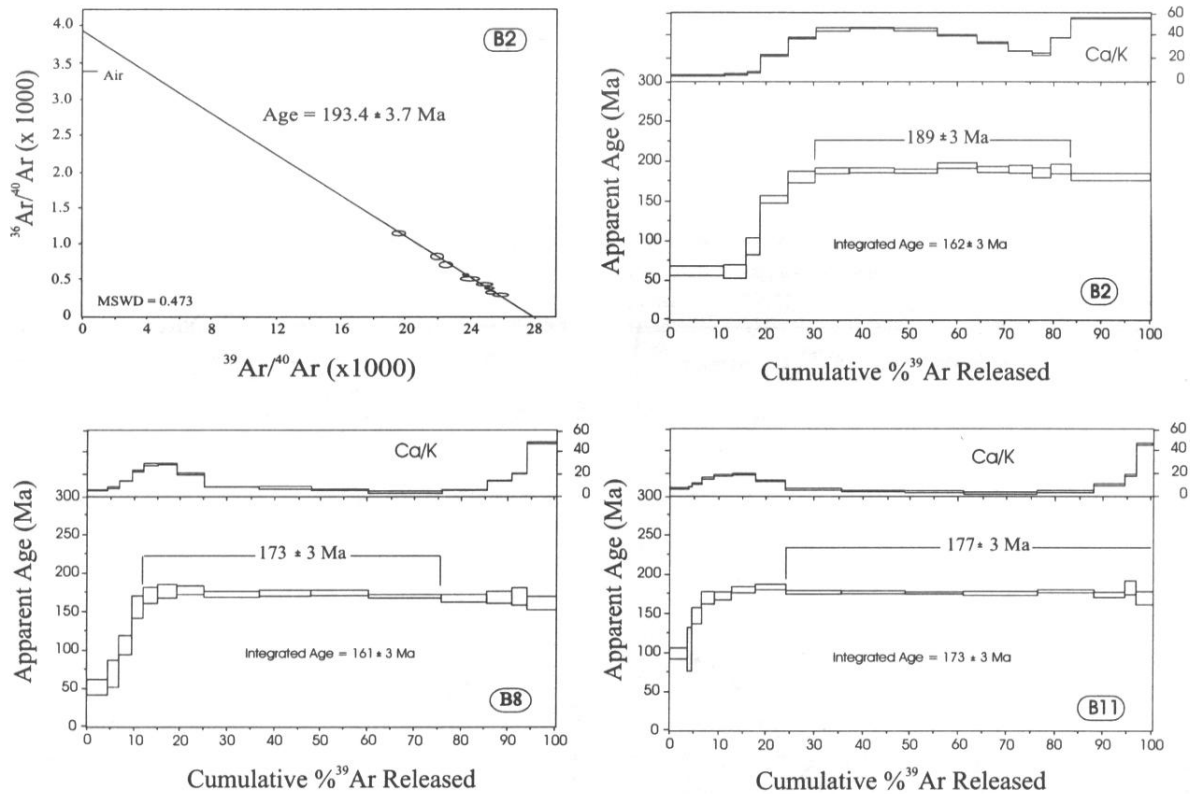


Figure 3. Inverse isochron ($^{36}\text{Ar}/^{40}\text{Ar}$ vs. $^{39}\text{Ar}/^{40}\text{Ar}$) of basalt B2, and $^{40}\text{Ar}/^{39}\text{Ar}$ apparent age spectra for plagioclase separates of samples B2, B8 and B11. Ca/K is calculated from $^{37}\text{Ar}/^{39}\text{Ar}$. MSWD (mean square weighted deviation) for B2 inverse isochron is 0.473. Analytical uncertainties are quoted at the 2σ confidence level.

within the range of Ar/Ar ages of other CAMP basalts [191–205 Ma; *Sebai et al.*, 1991; *Deckart et al.*, 1997; *Marzoli et al.*, 1999; *Hames et al.*, 2000].

Note that the biotite separate of the basement trondhjemite B3 yielded a well defined plateau age of $281 \pm 5 \text{ Ma}$, consistent with a late-Variscan crystallization.

6. WHOLE ROCK GEOCHEMISTRY

6.1. Major and Trace Elements

The analyzed rocks are low TiO_2 (0.94–1.02 wt%) CIPW quartz normative tholeiites (except olivine-normative sample B7; Table 1). According to the TAS diagram [*Le Bas et al.*, 1986] the Kerforne samples are classified as basalts (Fig. 4). The Mg# varies between 57.6 and 61.7, showing that the basalts are moderately evolved. Although major and trace element variations are moderate and mostly within analytical uncertainty within the whole dike, a relatively good correlation is observed

between decreasing MgO (8.2–7.3 wt%) versus increasing SiO_2 and Zr (with the exception of the dike margin B9). The correlation between MgO and other major and trace elements is not well defined (Fig. 5). Some incompatible elements, notably K_2O and Rb, display a relatively large variability (0.3–0.8 wt% for K_2O , and 15–25 ppm for Rb, c.f. Table 1).

On the multi-element mantle normalized diagram [*Sun and McDonough*, 1989] the Brittany tholeiites show an enrichment in the most incompatible trace elements (ITE; Fig. 6). The LILE (large ion lithophile elements, Rb, Ba, K) are the elements displaying the strongest variability. There is a significant negative Nb anomaly with respect to LILE and light rare earth elements (LREE). Similarly, Ti is slightly depleted compared to Zr and Y. Samples B1 and B5 show a rather marked positive Sr anomaly (mantle normalized $\text{Sr}/\text{Sr}^* = 1.65$ and 1.90, respectively), whereas B9 has a negative Sr anomaly (0.80).

The chondrite-normalized [cn; *Boynton*, 1984] REE display only minor variability along the whole dike (Fig. 7). The pattern is slightly light REE enriched ($\text{La}/\text{Yb}_{\text{cn}} =$

Table 3. Ar/Ar data for step heating analysis of sample B2. ⁴⁰Ar* = radiogenic ⁴⁰Ar. Temperature is given in °C. 2σ errors are shown and don't include uncertainties in J value. J = 0.003152

| Temperature °C | ⁴⁰ Ar/ ³⁹ Ar | ³⁷ Ar/ ³⁹ Ar | ³⁶ Ar/ ³⁹ Ar | ⁴⁰ Ar*/ ³⁹ Ar | % ⁴⁰ Ar* | ⁴⁰ Ar Moles | Age (Ma) | +/- |
|----------------|------------------------------------|------------------------------------|------------------------------------|-------------------------------------|---------------------|------------------------|----------|--------|
| 550 | 33.557 | 3.67275 | 7.75E-02 | 10.973 | 32.6 | 1.17E-14 | 61.344 | 5.568 |
| 600 | 24.769 | 4.136846 | 4.76E-02 | 11.075 | 44.6 | 1.47E-15 | 61.903 | 8.000 |
| 650 | 30.233 | 5.092685 | 4.81E-02 | 16.505 | 54.4 | 2.40E-15 | 91.495 | 10.377 |
| 700 | 43.491 | 15.7496 | 5.81E-02 | 27.936 | 63.5 | 1.19E-14 | 152.248 | 4.1844 |
| 750 | 50.211 | 25.8863 | 6.64E-02 | 33.323 | 65.1 | 1.32E-14 | 180.184 | 6.526 |
| 800 | 43.877 | 30.93122 | 4.19E-02 | 34.809 | 77.5 | 1.58E-14 | 187.811 | 3.519 |
| 850 | 41.329 | 31.78116 | 3.31E-02 | 34.965 | 82.6 | 1.93E-14 | 188.617 | 2.602 |
| 900 | 38.682 | 30.58637 | 2.39E-02 | 34.890 | 88.1 | 1.76E-14 | 188.232 | 2.415 |
| 950 | 38.883 | 27.41187 | 2.12E-02 | 35.564 | 89.6 | 1.65E-14 | 191.682 | 3.069 |
| 1000 | 38.365 | 23.16169 | 1.91E-02 | 35.218 | 90.2 | 1.23E-14 | 189.908 | 3.345 |
| 1050 | 38.107 | 18.14978 | 1.65E-02 | 35.168 | 91 | 8.53E-15 | 189.653 | 4.193 |
| 1100 | 39.477 | 16.13693 | 2.27E-02 | 34.488 | 86.3 | 6.79E-15 | 186.170 | 5.517 |
| 1200 | 35.687 | 20.09528 | 2.20E-02 | 31.272 | 86.3 | 1.01E-14 | 169.599 | 5.348 |
| 1300 | 41.023 | 25.81309 | 2.89E-02 | 35.254 | 84.3 | 6.89E-15 | 190.094 | 5.760 |
| 1601 | 43.986 | 37.77531 | 4.94E-02 | 33.382 | 73.7 | 3.89E-14 | 180.487 | 3.170 |

2.37-2.57) which is typical of CAMP tholeiites [Alibert, 1985; Dupuy et al., 1988; Bertrand, 1991; De Min et al., present volume]. A small Eu anomaly characterizes the analyzed samples (Eu/Eu*=0.90-0.96).

The major, trace and REE compositions of Kerforne basalts are similar to those of other European CAMP basalts, e.g., Pyrenees, and Messejana dike [Alibert, 1985; Beziat et al., 1991; Demant et al, 1996]. The mantle-normalized ITE patterns of Kerforne basalts are similar to those of most CAMP tholeiites (and CFB's in general), which also display a marked negative Nb anomaly. The REE patterns resemble those of South American and African low-TiO₂ CAMP basalts [De Min et al., present volume; Bertrand et al., 1982; Bertrand, 1991]. Compared to other CAMP tholeiites, the Kerforne basalts have among the lowest incompatible LILE and LREE enrichments and relatively low absolute ITE (including REE) concentrations.

6.2. Sr, Nd, Pb Isotopic Compositions

Initial ⁸⁷Sr/⁸⁶Sr and ¹⁴³Nd/¹⁴⁴Nd (recalculated to 200 Ma) display a moderate variation from 0.7053 to 0.7064 (ε_{Sr} between 15 and 30) and from 0.51232 to 0.51241 (ε_{Nd} from -1.22 to 0.55; Fig. 8; Table 4). The most radiogenic Sr isotopic composition belongs to sample B5, which appears to be slightly altered. However, its ¹⁴³Nd/¹⁴⁴Nd value (0.51239) is indistinguishable from those of the other samples. In general, the Sr-Nd isotopic composition of the dike suggests that the Kerforne basalts derived from a source enriched in radiogenic Sr

(i.e., with high time integrated Rb/Sr) and similar to the Bulk Silicate Earth (BSE) in terms of Nd isotopic composition (i.e., with chondrite-like REE pattern). In more detail, we observe a positive correlation between ε_{Sr} and ε_{Nd} (Fig. 9), i.e., the Kerforne samples define a trend which is different from that of the mantle array. No correlation is evident with MgO or Mg#.

The Sr-Nd isotopic compositions of Kerforne basalts fall within the field of other CAMP basalts [Dupuy et

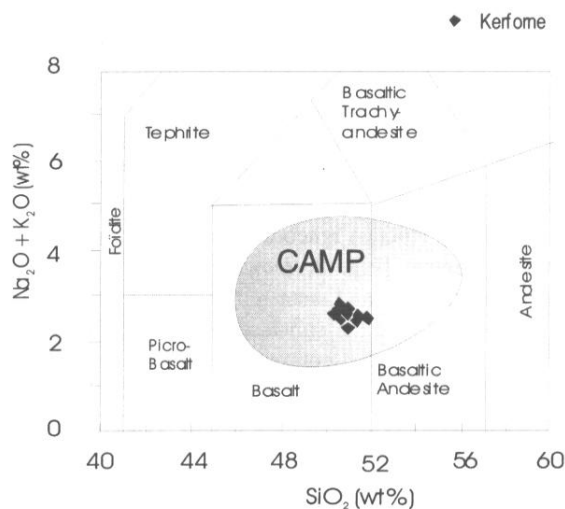


Figure 4. Total Alkalies-SiO₂ classification diagram [Le Bas et al., 1986] of Kerforne samples (black diamonds). The circled field represents compositions of published CAMP rocks [e.g., Alibert, 1985; Bertrand, 1991; McHone, 2000].

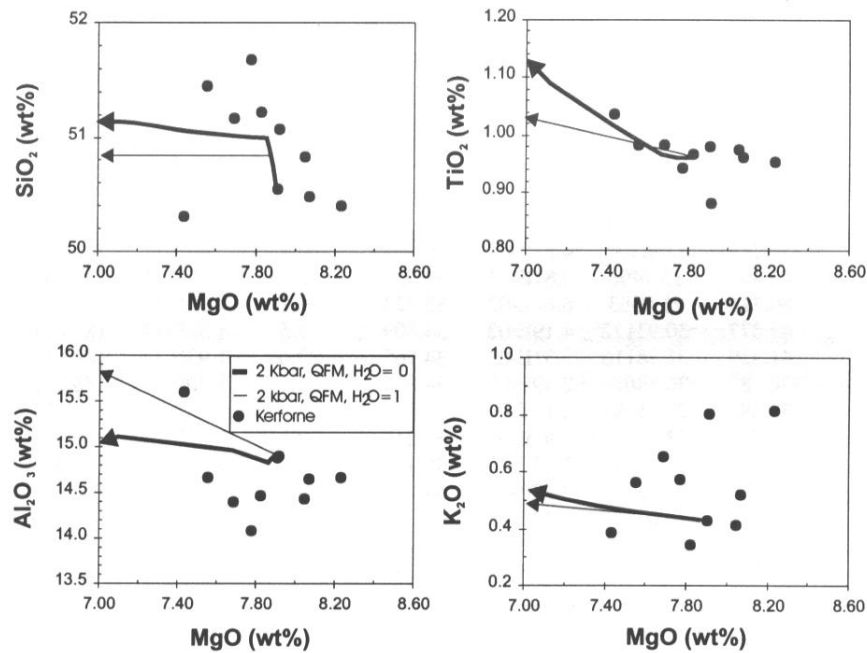


Figure 5. SiO_2 , TiO_2 , Al_2O_3 and K_2O vs. MgO variation diagrams for Kerforne samples. The bold and thin lines represent anhydrous and hydrous MELTS [Ghiorso and Sack, 1995] fractional crystallization modeling at low pressure (2 kbar) and $f\text{O}_2$ (QFM buffer) and with H_2O concentrations of 0 and 1.0 wt% in the starting magma (B2). Note that for major elements an analytical uncertainty of 1 wt% has to be considered.

al., 1988; Pegram, 1990; De Min *et al.*, present volume], and most closely resemble those of the Pyrenees and of the Iberian Messejana dike [Alibert, 1985; Fig. 8]. In general, initial (200 Ma) Sr-Nd isotopic compositions of CAMP basalts display a wide variation, from E-MORB to high ϵ_{Sr} and relatively low ϵ_{Nd} . The previously described trend of decreasing ϵ_{Sr} and ϵ_{Nd} for Kerforne basalts seems to depart from the composition of the few analyzed Pyrenean basalts and to be different from the main trend of CAMP basalts. In terms of Sr-Nd isotopic compositions, Kerforne basalts plot close to some lower crustal basic (meta-) igneous xenoliths from the French Massif Central [Fig. 8; Downes *et al.*, 1990, 1991], whereas granitoid and meta-sedimentary basement rocks from Brittany have a substantially more radiogenic Sr and unradiogenic Nd composition [Bernard-Griffiths *et al.*, 1985; cf. B3, Table 4; Fig. 8].

Initial (200 Ma) $^{206}\text{Pb}/^{204}\text{Pb}$ (18.20-18.37), $^{207}\text{Pb}/^{204}\text{Pb}$ (15.59-15.64) and $^{208}\text{Pb}/^{204}\text{Pb}$ (38.18-38.34) are roughly constant throughout the dike (Fig. 8). $^{206}\text{Pb}/^{204}\text{Pb}$ isotopic compositions are relatively unradiogenic, while $^{207}\text{Pb}/^{204}\text{Pb}$ and $^{208}\text{Pb}/^{204}\text{Pb}$ are slightly higher than those of MORBs or OIBs, i.e., higher than the Northern Hemisphere Reference Line [NHRL, Hart, 1984]. No correlation is evident between ϵ_{Sr} and ϵ_{Nd} and Pb isotopic com-

positions. In general, Pb isotopic compositions of Kerforne basalts plot within the field of CAMP basalts from Eastern North America [Pegram, 1990]. Such compositions resemble those of lower crustal basic (meta-) igneous xenoliths from the Massif Central [Downes *et al.*, 1991; Fig. 8].

Finally, we note the difference between the Sr-Nd-Pb isotopic compositions of Kerforne basalts (and of the CAMP in general) compared to those of Ocean Island Basalts (OIB) from the Central Atlantic islands of Cape Verde, Fernando de Noronha and Ascension [e.g. Gerlach *et al.*, 1987, 1988; Davies *et al.*, 1985; Halliday *et al.*, 1992; Fig. 8] which have been suggested to be the present day expression of the hot spot source which generated CAMP basalts [Wilson, 1997; Leitch *et al.*, 1998].

7. PETROGENESIS OF KERFORNE BASALTS.

7.1. Fractional Crystallization

Kerforne basalts are moderately evolved, as they have MgO , Cr and Ni which are too low to be considered primary or near-primary mantle melts. According to MELTS [Ghiorso and Sack, 1995] calculations, Kerforne basalts may result from 30-40% fractional crystallization

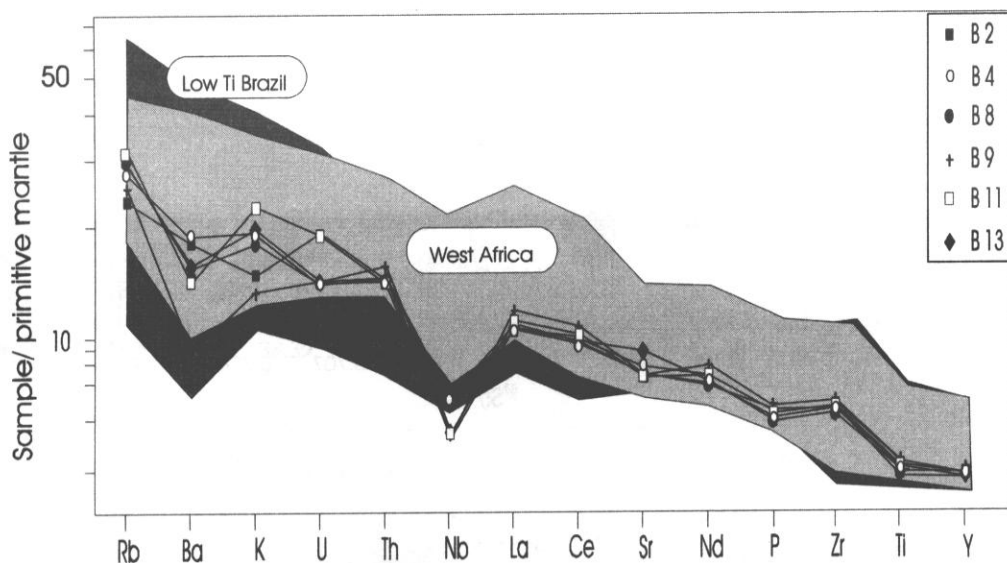


Figure 6. Primitive mantle normalized [Sun and McDonough, 1989] incompatible trace elements patterns for representative selected Kerforne basalts. Low TiO₂ CAMP rocks from Brazil [De Min et al., present volume] and West Africa [Bertrand, 1991] are represented by the dark and light gray fields, respectively.

of olivine, minor cpx and spinel, starting from a primitive magma [e.g., Hirose and Kushiro, 1993]. Depending on the selected run conditions (pressure between 0.5 and 8 kbar, H₂O between 0 and 1 wt%; fO₂ either at the QFM or NNO buffer), the differentiation from less to more evolved Kerforne basalts (Mg# 62-58) would require 10-16 wt% fractionation of a gabbroic assemblage (augite, plagioclase and magnetite ± pigeonite ± olivine). However, the observed MgO vs. Al₂O₃ and K₂O trends of Kerforne basalts do not match the calculated trends (Fig. 5), which may be due to slightly lower crustal contamination and/or weak hydrothermal alteration of the samples.

7.2. Alteration and Crustal Assimilation

The sericitization that affected the plagioclase rims is evidence of a post-magmatic hydrothermal alteration which may have increased the K₂O (and Rb and Ba?) concentration of the basalts. There is some evidence that few samples (B1 and B5) have a positive Sr anomaly, and the Sr isotopic composition of B5 falls off the field of other Kerforne basalts (Table 4). It may be argued that the Sr concentration and isotopic composition of B5 is altered (i.e., enriched) by post-magmatic processes, even if samples were acid-leached before isotopic analyses. In general, however, no correlation is observed between Sr concentrations and Sr-Nd isotopic compositions; i.e., samples with similar ε_{Sr} (e.g., B8 and B13) have different

Sr concentration (167 and 194 ppm, respectively; Table 1 and 4). In any case, it is unlikely that alteration (and weathering) affected the composition of the generally immobile REE, and therefore ε_{Nd} (cf., Foland et al., 2000). In fact, ε_{Nd} of B5 falls within the field of the other analyzed basalts.

The positive ε_{Nd}-ε_{Sr} trend of Kerforne basalts is different from mantle-generated oceanic and continental ba-

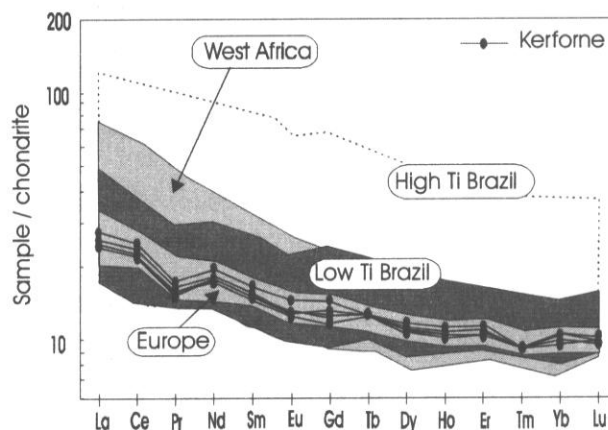


Figure 7. Chondrite-normalized [Boynton, 1984] REE compositions of Kerforne and CAMP basalts from Europe [Alibert, 1985; Demant et al., 1996] West Africa [Bertrand, 1991], and Brazil [low and high TiO₂ samples; De Min et al., present volume].

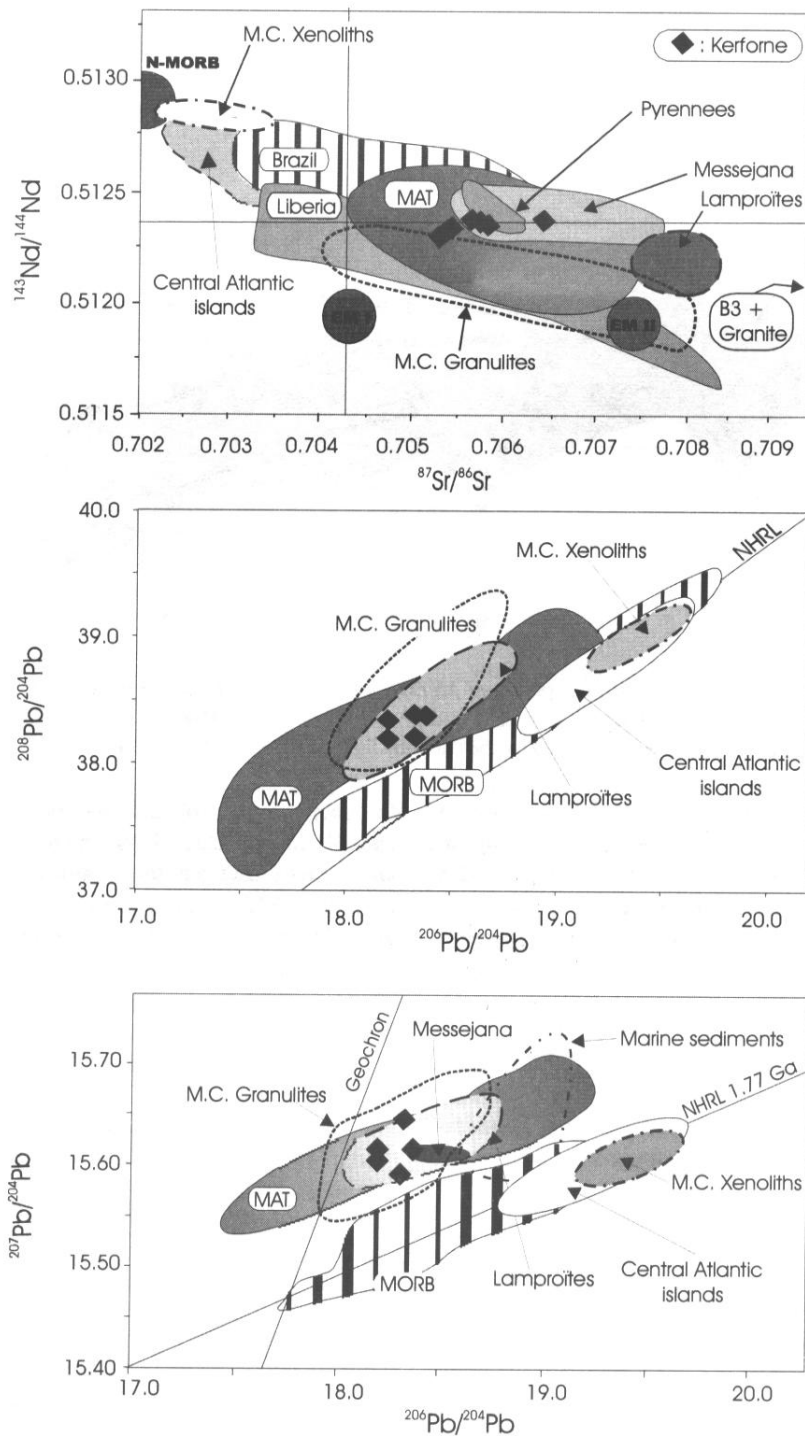


Figure 8. Initial (200 Ma) Sr, Nd and Pb isotopic compositions of Kerforne basalts (black diamonds) and of other CAMP basalts from Europe [Pyrenees and Messejana dike; *Alibert, 1985*], West Africa [*Dupuy et al., 1988*], Brazil [*De Min et al., present volume*] and Eastern North America [Mesozoic Appalachian Tholeiites, MAT; *Pegram, 1990*]. Isotopic compositions (recalculated to 200 Ma) of granulites from the Massif Central [*Downes et al., 1990, 1991*], mantle xenoliths from the Massif Central [*Zangana et al., 1997*] and lamproites from western Brittany [*Turpin et al., 1988*] are contoured by a dotted, a dotted-dashed and a dashed line, respectively. Mantle poles after *Zindler and Hart [1986]* and *Sun and McDonough [1989]*. Marine sediments after *Pegram [1990]*, Atlantic oceanic islands (Cape Verde, Fernando da Noronha and Ascension) after *Gerlach et al. [1987, 1988]*, *Davies et al. [1989]*, *Halliday et al. [1992]*. Sr-Nd compositions of granitic rocks from Brittany [B3, and *Bernard Griffiths et al., 1985*] are located out of the figure and are indicated by an arrow.

Table 4. Measured and initial (200 Ma) Pb-Sr-Nd isotopic compositions of selected Kerforne basalts and of one wall-rock sample (B3). Initial ϵ_{Sr} and ϵ_{Nd} are indicated. Analytical uncertainty is quoted at the 2σ level, which, for Pb isotopic analyses is less than 0.01.

| sample | Kerforne basalts | | | | | | granite B3 |
|-----------------------|------------------|---------------|---------------|--------------|--------------|--------------|---------------|
| | B2 | B5 | B8 | B9 | B11 | B13 | |
| $^{206}Pb/^{204}Pb_m$ | 18.52 | 18.39 | 18.52 | 18.40 | 18.51 | - | 19.32 |
| $^{206}Pb/^{204}Pb_i$ | 18.32 | 18.31 | 18.37 | 18.20 | 18.20 | - | 18.89 |
| $^{208}Pb/^{204}Pb_m$ | 38.55 | 38.39 | 38.54 | 38.40 | 38.51 | - | 37.98 |
| $^{208}Pb/^{204}Pb_i$ | 38.36 | 38.18 | 38.34 | 38.19 | 38.31 | - | 37.89 |
| $^{207}Pb/^{204}Pb_m$ | 15.65 | 15.60 | 15.63 | 15.62 | 15.62 | - | 15.62 |
| $^{207}Pb/^{204}Pb_i$ | 15.64 | 15.59 | 15.62 | 15.61 | 15.61 | - | 15.59 |
| $^{87}Sr/^{86}Sr_m$ | 0.705946 (7) | 0.707225 (11) | 0.706521 (7) | 0.706172 (6) | 0.706612 (7) | 0.706544 (7) | 0.711821 (9) |
| $^{87}Sr/^{86}Sr_i$ | 0.705305 | 0.706389 | 0.705762 | 0.705388 | 0.705740 | 0.705858 | 0.709234 |
| ϵ_{Sr} | 14.77 | 30.16 | 21.26 | 15.95 | 20.95 | 22.63 | 70.56 |
| $^{143}Nd/^{144}Nd_m$ | 0.512541 (21) | 0.512612 (12) | 0.512591 (12) | 0.512569 (8) | 0.512554 (4) | 0.512564 (8) | - |
| $^{143}Nd/^{144}Nd_i$ | 0.512318 | 0.512389 | 0.512370 | 0.512349 | 0.512409 | 0.512351 | - |
| ϵ_{Nd} | -1.22 | 0.17 | -0.20 | -0.62 | 0.55 | -0.58 | - |

salts, including other CAMP basalts. Therefore, the Kerforne Sr-Nd isotopic compositions may have been modified during interaction with the continental crust. A possible assimilant would be the silicic upper crust, including the dike wall-rocks. However, the silicic basement rocks in western Brittany (including the here analyzed trondjemite B3) are at least of Variscan age (i.e., Early Permian to Cambrian) and are characterized by negative ϵ_{Nd} and by high ϵ_{Sr} (Fig. 8) and therefore can not explain the ϵ_{Sr} - ϵ_{Nd} correlation of Kerforne basalts. Moreover, contamination with the silicic crust would substantially increase, for example, the SiO_2 content, which is not observed for Kerforne basalts that are, among CAMP basalts, relatively SiO_2 -poor.

Alternatively, it could be suggested that the basaltic magma interacted with a mafic (lower) crust having negative ϵ_{Nd} and low ϵ_{Sr} . Outcrops of the lower crust are absent in Brittany, but basic (meta-) igneous xenoliths are present in Cenozoic alkaline volcanic rocks of the Massif Central, central France [Downes *et al.*, 1990, 1991]. These (meta-) igneous rocks were formed by deep crustal basaltic intrusions or metamorphism, probably during the Variscan orogeny. Some of these mafic rocks are characterized by moderately negative ϵ_{Nd} , moderately positive ϵ_{Sr} and high $^{207}Pb/^{204}Pb$ (Fig. 8).

In general, isotopic compositions do not correlate with major (e.g., SiO_2 and MgO) and trace elements. How-

ever, the basalts having the lowest ϵ_{Nd} (e.g., B2 and B9) contain a few plagioclase aggregates which are characterized by rounded high-An (bytownite) cores, quite different from the other microphenocrysts and microlites (An_{75-42}). The apparent textural and chemical disequilibrium of the high-An plagioclase cores suggests that they are xenocrysts in the Kerforne basalts. Modeling of incompatible minor elements, suggests that the high-An plagioclase cores may have crystallized at equilibrium from an MgO-rich and K_2O -poor, mafic magma.

Assimilation of mafic lower crustal rocks by CFBs has been proposed for example for some Deccan trap forma-

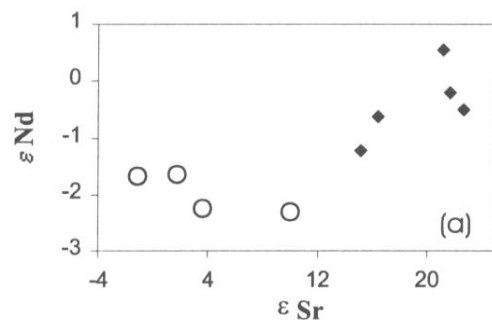


Figure 9. Detail of Sr-Nd isotopic composition of Kerforne basalts (diamonds) and of some Massif Central mafic xenoliths [white circles; Downes *et al.*, 1990].

tions [Peng *et al.*, 1994], and evidence of interaction between basaltic magma and the lower crust have been described for example for the deep crust section in the Ivrea zone [e.g., Sinigoi *et al.*, 1995]. Reiners *et al.* [1995] have shown that during initial stages of crystallization, a basaltic magma is capable of assimilating large amounts of granite. Performing isenthalpic MELTS runs, it can be shown that at lower crustal depths a primitive basaltic magma is capable of assimilating 10-15 wt% of a relatively hot (e.g., 800 °C) mafic granulitic wall rock (60% plagioclase + cpx + opx ± garnet), without substantially changing his basaltic composition.

In summary, Kerforne basalts were not substantially contaminated by Variscan or pre-Variscan upper silicic crust, but may have interacted with basic lower crust and may even have entrained plagioclase xenocrysts from it. Consequently, it may be concluded that the highest ϵ_{Sr} and ϵ_{Nd} (+23 and +0.55, respectively) of unaltered Kerforne basalts are close to the Sr-Nd isotopic composition of their mantle source. This mantle source may have been slightly enriched in Rb/Sr, compared to a primitive mantle, and may have had a near-chondritic REE pattern.

8. THE MANTLE SOURCE OF KERFORNE BASALTS

8.1. REE Constraints

The moderately evolved Kerforne basalts display a slightly LREE enriched pattern with no significant Eu anomaly (Fig. 7). Such a pattern is typical of most CAMP rocks and may result from a differentiation process which involved: (a) melting of a mantle peridotite; (b) fractional crystallization dominated by olivine and (c) possible assimilation of mafic lower crust. We assume that the role of assimilation of mafic crustal rocks, which have low REE concentrations and LREE/HREE values similar to the basalts [Downes *et al.*, 1990], was negligible. Equilibrium melting and fractional crystallization have been modeled by using standard equations [Shaw, 1967; and Rayleigh fractionation], and considering the parameters (modal compositions, melting and partition coefficients) reported in the caption of Fig. 10. The inferred initial REE concentrations of the mantle peridotite are either chondritic or slightly enriched, as is suggested by the ϵ_{Nd} compositions of Kerforne basalts.

The moderately LREE-enriched pattern of Kerforne basalts cannot be due to equilibrium melting of a spinel peridotite or of a garnet peridotite for initial source compositions being either chondritic or slightly enriched (Fig. 10). This is striking for La/Yb vs. Gd/Yb of the basalts (Fig. 10b). The discrepancy between calculated and ob-

served REE ratios can not be explained by the fact that Kerforne basalts are not primitive, since fractional crystallization (± assimilation of a mafic rock) does not substantially change the La/Yb and Gd/Yb.

The REE compositions and ratios of Kerforne basalts are better reproduced by 11-13% equilibrium melting of a slightly enriched garnet + spinel peridotite and subsequent 20-30% fractional crystallization of olivine + cpx (Fig. 10). The slightly enriched nature of the modeled source is consistent with the close to chondritic Nd isotopic composition of the basalts.

8.2. Isotopic Constraints

In terms of Sr-Nd-Pb isotopic composition, Kerforne basalts are substantially different (i.e., enriched in ϵ_{Sr}) compared to those of oceanic basalts, but similar to those of most basalts from the CAMP and other CFB provinces. Generally, it has been suggested that the high ϵ_{Sr} of CFBs is due to assimilation of crustal material and/or to melting of an enriched continental lithospheric mantle. For Kerforne basalts, we suggest that crustal contamination with high ϵ_{Sr} material (upper crust) and hydrothermal alteration was negligible (except for outlier sample B5). The high Sr isotopic composition of Kerforne basalts (i.e., B13) may therefore be the closest estimate of their mantle source composition.

The composition of the continental lithosphere is known either from mantle xenoliths or from basaltic rocks of clear lithospheric origin. Samples of nearby lithospheric mantle are represented by spinel peridotite xenoliths entrained by Cenozoic alkali basalts of the Massif Central. Although these xenoliths may not be representative of the most fertile lithosphere. Their REE pattern are either depleted or substantially enriched in LREE [Zangana *et al.*, 1997; Lenoir *et al.*, 2000]. These peridotites have negative ϵ_{Sr} and positive ϵ_{Nd} and Pb isotopic compositions plotting on the NHRL [Zangana *et al.*, 1997]. Therefore, Massif Central mantle xenoliths are not a suitable mantle source for Kerforne basalts.

Late Variscan lamproites spread out over France, including western Brittany (Fig. 1) are witness of a strongly enriched and fertile lithosphere. These uncontaminated magmas were probably generated by melting of portions of the continental lithospheric mantle enriched by recycling of crustal material during the Variscan orogeny [Turpin *et al.*, 1988]. These lamproites have an incompatible element pattern which is similar in shape to those of Kerforne basalts, although substantially more enriched, with about 100 times chondritic LREE and LILE and relatively depleted HFSE (Ta) and Ti [Turpin *et al.*, 1988]. Their isotopic compositions are similar to those of

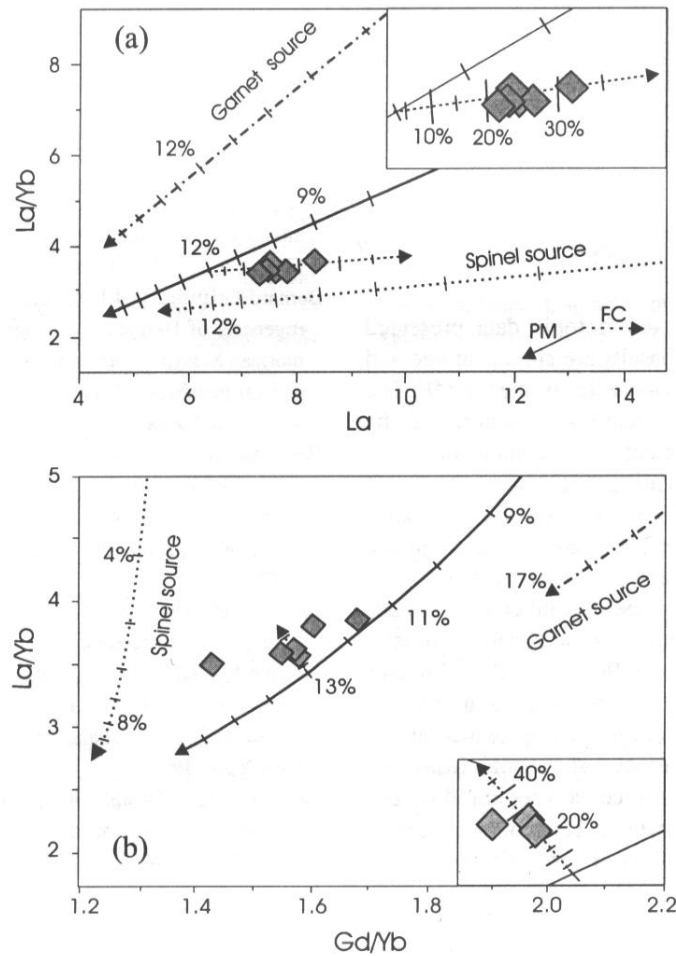


Figure 10. La/Yb vs. La and La/Yb vs. Gd/Yb compositions of Kerforne basalts and various peridotite melting models. Spinel + garnet peridotite melting: solid line; garnet peridotite melting: dashed line; spinel peridotite melting: dotted line. Small numbers close to melting curves represent melting percent. Modal composition of the peridotite: olivine = 55%, orthopyroxene = 25%, clinopyroxene = 15%, spinel and/or garnet = 5%. Initial composition (ppm) of the spinel and garnet peridotite: La = 0.78, Gd = 0.4; Eu = 0.11 and Yb = 0.34. Partition coefficients are from *McKenzie and O'Nions* [1991]. Fractional crystallization (dashed line, and inset of Fig. 10b) has been calculated considering the fractionating minerals calculated by MELTS for hydrous (1 wt% H₂O), low pressure (2 kbars) and QFM conditions.

Kerforne basalts for Pb, but different for Sr and Nd (Fig. 8). Although the similarity of the ITE pattern and of the Pb isotopic composition is striking, it is obvious that Kerforne basalts were not entirely generated by a mantle source similar to that of the lamproites. We suggest however, that a mantle component, similar to the "lamproitic source" may have contributed to the enriched isotopic signature of Kerforne basalts.

Contamination of magmas originating in the asthenosphere with enriched lithospheric mantle components has been proposed also for other CFB provinces, notably the Karoo [e.g., *Ellam and Cox*, 1991; *Luttinen and Furnes*,

2000]. Similarly, it has been suggested that CAMP basalts from Eastern North America were generated from a mantle source enriched by subducted oceanic sediments [*Pegram*, 1990].

Assuming that the "lamproitic" source represented the enriched mantle signature, a mantle with low ϵ_{Sr} , close to primitive ϵ_{Nd} and high $^{207}\text{Pb}/^{204}\text{Pb}$ is required to contribute to the origin of Kerforne basalts. Such a component may correspond to the bulk silicate earth (BSE), as calculated by *Allegre et al.* [1988]. We note that neither the lithospheric mantle xenoliths from the Massif Central [*Zangana et al.*, 1997] nor OIBs of the Central Atlantic

(e.g., Cape Verde, Fernando de Noronha or Ascension) fit the required Sr-Nd and particularly Pb isotopic compositions (Fig. 8). Note that these ocean islands have been suggested to be the present-day expression of the mantle-plume which may have generated CAMP [Hill, 1991; Wilson, 1997; Leitch *et al.*, 1998].

9. CONCLUSIONS

The Ar/Ar, geochemical and isotopic data presented here confirm that Kerforne basalts are similar in age and composition to the low-TiO₂ tholeiites of the CAMP. The Kerforne dike is the northernmost known outcrop of the CAMP, even if its emplacement is not demonstrably related to the Central Atlantic rifting (Fig. 1).

Based on petrographic, mineralogic and isotopic data, we argue that the basaltic Kerforne magmas were slightly contaminated with mafic lower crust, but were probably not substantially affected by upper crustal contamination. The "uncontaminated" endmember of Kerforne basalts points to relatively radiogenic Sr and ²⁰⁷Pb/²⁰⁴Pb and close to chondritic Nd isotopic compositions, shared also by the other basalts of the European sub-province of the CAMP. This suggests the presence of an isotopically enriched lithospheric mantle source component different from typical OIB or MORB mantle. This component may have been similar to that from which the Carboniferous lamproites of western Brittany originated. By contrast, it is unlikely that Kerforne magmas were generated only from a mantle source similar to the isotopically depleted continental lithosphere, as represented by mantle xenoliths from the Massif Central, nor from a mantle source similar to OIBs of the Central Atlantic (Cape Verde, Fernando de Noronha or Ascension). We speculate that Kerforne magmas may have been generated from a sub-lithospheric BSE-like mantle and were enriched en route to the surface first by "lamproitic" portions of the continental lithosphere and subsequently contaminated by the mafic lower crust.

Acknowledgments. J.L. Malfère (isotope analyses), S. Beuchat (XRD), D. Giorgis (Ar/Ar dating), and F. Bussy (electron microprobe), are thanked for analytical assistance. Discussions with M. A. Dungan, L. Melluso, E. M. Piccirillo, P. R. Renne, and C. Rapaille helped to improve the manuscript as well as critical reviews by A.L. Heatherington, and an anonymous reviewer. Editorial assistance by J.G. McHone was particularly appreciated. Financial support from the Swiss Science Foundation (grant FNRS 2100-057218.99 to A. M.) is acknowledged.

REFERENCES

- Alibert, C., A Sr-Nd isotope and REE study of the late Triassic dolerites from the Pyrenees (France) and the Messejana dyke (Spain and Portugal), *Earth Planet. Sci. Lett.*, 73, 81-90, 1985.
- Allègre, C.J., E. Lewin, and B. Dupré, A coherent crust-mantle model for the uranium-thorium-lead isotopic system, *Chem. Geol.*, 70, 211-234, 1988.
- Bernard-Griffiths, J., J.J. Peucat, S. Sheppard, and P. Vidal, Petrogenesis of Hercynian leucogranites from the Southern Armorican Massif: contribution of REE and isotopes (Sr, Nd, Pb and O) geochemical data to the study of source rock characteristics and ages, *Earth Planet. Sci. Lett.*, 235-250, 1985.
- Bertrand, H., Le magmatisme tholéiitique continental de la marge ibérique, précurseur de l'ouverture de l'Atlantique central: les dolerites du dyke de Messajana-Plasencia (Portugal-Espagne). *C. R. Acad. Sc. Paris*, 304, 215-220, 1987.
- Bertrand, H., The Mesozoic tholeiitic province of northwest Africa: a volcano-tectonic record of the early opening of the Central Atlantic, in *Magmatism in extensional structural setting (the Phanerozoic African plate)*, edited by A.B. Kampunzu and R.T. Lubala, pp. 147-191, Springer, Heidelberg, New York, 1991.
- Bertrand, H., J. Dostal, and C. Dupuy, Geochemistry of Early Mesozoic tholeiites from Morocco, *Earth Planet. Sci. Lett.*, 58, 225-239, 1982.
- Bertrand, H., J. Liegeois, K. Deckart, and G. Feraud, High-Ti tholeiites in Guiana and their Connection with the Central Atlantic CFB Province: Elemental and Sr-Nd-Pb Isotopic Evidence for a Preferential Zone of Mantle Upwelling in the Course of Rifting, in *Spring Meeting*, edited by AGU, 1999.
- Béziat, D., J.L. Joron, P. Monchoux, M. Treuil, and F. Walgenwiz, Geodynamic implication of geochemical data for the Pyrenean ophiolites (Spain-France), *Chem. Geol.*, 243-262, 1991.
- Bindeman, I.N., A.M. Davis, and M.J. Drake, Ion microprobe study of plagioclase-basalt partition experiments at natural concentration levels of trace elements, *Geochim. Cosmochim. Acta*, 62, 1175-1193, 1998.
- Boynnton, W.V., Geochemistry of the rare earth elements: meteorite studies, in *Rare earth element geochemistry*, edited by P. Henderson, pp. 63-114, Elsevier, 1984.
- Caroff, M., H. Bellon, L. Chauris, J.P. Carron, S. Chevrier, A. Gardinier, J. Cotten, Y. Le Moan, and Y. Neidhart, Magmatisme fissural Triasico-Liasique dans l'ouest du massif armoricain (France) : pétrologie, géochimie, âge et modalité de mise en place, *Can. J. Earth Sci.*, 32, 1921-1936, 1995.
- Caroff, M., X. Le Gal, and J. Rolet, Magmatisme tholéiitique continental en contexte orogénique hercynien : l'exemple du

- volcanisme viséen de Kerroc'h, massif armoricain (France), *C. R. Acad. Sci. Paris*, 322, 269-275, 1996.
- Davies, G.R., A. Gledhill, and C. Hawkesworth, Upper crustal recycling in southern Britain: evidence from Nd and Sr isotopes, *Earth Planet. Sci. Lett.*, 75, 1-12, 1985.
- Davies, G.R., M.J. Norry, D.C. Gerlach, and R.A. Cliff, A combined chemical and Pb-Sr-Nd isotope study of the Azores and Cape Verde hot spots: the geodynamic implication, in *Magmatism in the ocean basins*, edited by A.D. Saunders and M.J. Norry, pp. 231-255, Blackwell, Oxford, 1989.
- Deckart, K., G. Féraud, and H. Bertrand, Age of Jurassic continental tholeiites of French Guyana, Surinam and Guinea: implications for the initial opening of the Central Atlantic Ocean, *Earth Planet. Sci. Lett.*, 150, 205-220, 1997.
- Demant, A., and D. Morata, Les dolérites tholéiitiques de Gaujacq et St-Pandelon (Landes, France). Pétrologie, géochimie et cadre géodynamique, *Bull. Soc. Geol. France*, 167, 321-333, 1996.
- De Min, A., E. M. Piccirillo, A. Marzoli, G. Bellieni, P. R. Renne, M. Ernesto and L. S. Marques, The Central Atlantic Magmatic Province (CAMP) in Brazil: petrology, geochemistry, $^{40}\text{Ar}/^{39}\text{Ar}$ ages, paleomagnetism and geodynamic implications, Present Volume.
- Downes, H., C. Dupuy, and A.F. Leyreloup, Crustal evolution of the Hercynian belt of Western Europe: Evidence for lower-crustal granulitic xenoliths (French Massif Central), *Chem. Geol.*, 83, 209-231, 1990.
- Downes, H., P.D. Kempton, D. Briot, R.S. Harmon, and A.F. Leyreloup, Pb and O isotope systematics in granulite facies xenoliths, French Massif Central: implication for crustal processes, *Earth Planet. Sci. Lett.*, 102, 342 - 357, 1991.
- Dupuy, C., J. March, J. Dostal, A. Michard, and S. Testa, Asthenospheric and lithospheric source for Mesozoic dolerites from Liberia (Africa): trace element and isotope evidence, *Earth Planet. Sci. Lett.*, 87, 100-110, 1988.
- Ellam, R.M., and K.G. Cox, An interpretation of Karoo picrite basalts in terms of interaction between asthenospheric magmas and the mantle lithosphere, *Earth Planet. Sci. Lett.*, 105, 330-342, 1991.
- Foland, K.A., F.G.F. Gibb, and C.M.B. Henderson, Patterns of Nd and Sr isotopic ratios produced by magmatic and post-magmatic processes in the Shiant Isles Main Sill, Scotland., *Contr. Min. Pet.*, 139, 655-671, 2000.
- Gerlach, D.C., J.C. Stomer, and P.A. Mueller, Isotopic geochemistry of Fernando de Noronha, *Earth Planet. Sci. Lett.*, 85, 129-144, 1987.
- Gerlach, D.C., R.A. Cliff, G.R. Davies, M. Norry, and N. Hodgson, Magma source of the Cape Verde archipelago: isotopes and trace element constrains, *Geochim. Cosmochim. Acta*, 52, 2979-2992, 1988.
- Ghiorso, M.S., and R.O. Sack, Chemical mass transfer in magmatic processes IV. A revised and internally consistent thermodynamic model for the interpolation and extrapolation of liquid-solid equilibria in magmatic systems at elevated temperatures and pressures, *Contr. Min. Pet.*, 119, 197-212, 1995.
- Halliday, A.N., R.D. Gareth, S. Tommasini, C.R. Paslik, J.G. Fitton, and D.E. James, Lead isotope evidence for young trace element enrichment in the oceanic upper mantle, *Nature*, 359, 623-627, 1992.
- Hames, W. E., C. Ruppel, P. R. Renne, New evidence for geologically instantaneous emplacement of earliest Jurassic Central Atlantic magmatic province basalts on the North American margin, *Geology*, 28, 859-862, 2000.
- Hart, S.R., A large scale isotopic anomaly in the southern hemispheric mantle, *Nature*, 309, 753-757, 1984.
- Hergt, J.M., D.W. Peate, and C.J. Hawkesworth, The petrogenesis of Mesozoic Gondwana low-Ti flood basalts, *Earth Planet. Sci. Lett.*, 105, 134-148, 1991.
- Hill, R.I., Starting plume and continental break-up, *Earth Planet. Sci. Lett.*, 398-416, 1991.
- Hirose, K., and I. Kushiro, Partial melting of dry peridotites at high pressures: determination of compositions of melts segregated from peridotite using aggregates of diamond, *Earth Planet. Sci. Lett.*, 114, 477-489, 1993.
- Le Bas, M.J., R.W. Le Maitre, A. Streickeisen, and B. Zanettin, A chemical classification of volcanic rocks based on the total alkali silica diagram, *J. Pet.*, 27, 745-750, 1986.
- Leitch, A.M., G.F. Davies, and M. Wells, A plume head melting under a rifting margin, *Earth Planet. Sci. Lett.*, 161, 161-177, 1998.
- Lenoir, X., C. Garrido, J.L. Bodinier, and J.M. Dauria, Contrasting lithospheric mantle domains beneath the Massif Central (France) revealed by geochemistry of peridotite xenoliths, *Earth Planet. Sci. Lett.*, 181, 359-375, 2000.
- Lindsley, D.H., Pyroxene thermometry, *Am. Mineral.*, 68, 477-483, 1983.
- Luttinen, A.V., and H. Furnes, Flood basalts of Vestfjella: Jurassic magmatism across an Archean-Proterozoic lithospheric boundary in Dronning Maud Land, Antarctica, *J. Pet.*, 41, 1271-1305, 2000.
- Marzoli, A., P. Renne, E. Piccirillo, M. Ernesto, G. Bellieni, and A. De Min, Extensive 200-million-year-old continental flood basalts of the Central Atlantic Magmatic Province, *Science*, 284, 616-618, 1999.
- Matte, P., Tectonics and plate tectonic model for the Variscan Belt of Europe, *Tectonophys.*, 126, 329-374, 1986.
- McHone, J.G., Non-plume magmatism and rifting during the opening of the Central North Atlantic Ocean, *Tectonophys.*, 316, 287-296, 2000.
- McKenzie, D., and R.K. O'Nions, Partial Melt Distribution from Inversion of Rare Earth Element Concentrations, *J. Pet.*, 32, 1021-1091, 1991.
- Moreau, M.G., J.Y. Berthou, and J.A. Malod, New paleomagnetic Mesozoic data from the Algarve (Portugal): fast rotation

- of Iberia between the Hauterivian and the Aptian, *Earth Planet. Sci. Lett.*, 146, 689-701, 1997.
- Nimis, P., A clinopyroxene geobarometer for basaltic systems based on crystal-structure modeling, *Contrib. Min. Pet.*, 121, 1115-125, 1995.
- Onstott, T.C., M.L. Miller, R.C. Ewing, G.W. Arnold, and D.W. Alsh, Recoil refinements: implication for the $^{40}\text{Ar}/^{39}\text{Ar}$ dating technique, *Geochim. Cosmochim. Acta*, 59, 1821-1834, 1995.
- Panjasawatwong, Y., L.V. Danyushevsky, A.J. Crawford, and K.L. Harris, An experimental study of the effects of melt composition on plagioclase-melt equilibria at 5 and 10 kbar: implications for the origin of magmatic high-An plagioclase, *Contr. Min. Pet.*, 118, 420-432, 1995.
- Pegram, W.J., Development of continental lithospheric mantle as reflected in the chemistry of the Mesozoic Appalachian Tholeiites, U.S.A., *Earth Planet. Sci. Lett.*, 97, 316-330, 1990.
- Peng, Z.W., J. Mahoney, P. Hooper, C. Harris, and J. Beane, A role for lower continental crust in flood basalt genesis? Isotopic and incompatible element study of the lower six formations of the western Deccan Traps, *Geochim. Cosmochim. Acta*, 58, 267-288, 1994.
- Reiners, P.W., B. Nelson, and M.S. Ghiorso, Assimilation of felsic crust by basaltic magma; thermal limits and extents of crustal contamination of mantle derived magmas, *Geology*, 23, 563-566, 1995.
- Renne, P. R., C. C. Swisher, A. L. Deino, B. B. Karner, T. Owens and D. J. De Paolo, Intercalibration of Standards, Absolute ages and uncertainties in $^{40}\text{Ar}/^{39}\text{Ar}$ dating, *Chem. Geol.*, 145, 117-152, 1998.
- Rhodes, J.M., Geochemistry of Mauna Loa eruption: implication for magma storage and supply, *J. Geophys. Res.*, 93, 4453-4466, 1988.
- Sebai, A., G. Féraud, H. Bertrand, and J. Hanes, $^{40}\text{Ar}/^{39}\text{Ar}$ dating and geochemistry of tholeiitic magmatism related to the early opening of the Central Atlantic rift, *Earth Planet. Sci. Lett.*, 104, 45-472, 1991.
- Shaw, D.M., Trace element fractionation during anatexis, *Geochim. Cosmochim. Acta*, 34, 237-243, 1967.
- Sichler, B., and M. Perrin, New early Jurassic paleopole from France and Jurassic apparent polar wander, *Earth Planet. Sci. Lett.*, 115, 13-27, 1993.
- Sinigoi, S., J.E. Quick, A. Mayer, and G. Demarchi, Density-controlled assimilation of underplated crust, Ivrea-Verbano zone, Italy., *Earth Planet. Sci. Lett.*, 129, 183-192, 1995.
- Stampfli, G.M., J. Mosar, A. De Bono, and I. Vavasis, Late Paleozoic Early Mesozoic plate tectonics of the Western Tethys, *Bull. Geol. Soc. Greece*, 32, 113-120, 1998.
- Steiger, R.H., and E. Jäger, Subcommittee on geochronology: convention on the use of decay constants in geo and cosmochronology, *Earth Planet. Sci. Lett.*, 36, 359-362, 1977.
- Sun, S.S., and W.F. McDonough, Chemical and isotopic systematics of oceanic basalts: implication for mantle composition and processes, in *Magmatism in the ocean basins*, edited by A.D. Saunders and M.J. Norry, pp. 313-345, Blackwell, Oxford, 1989.
- Turpin, L., D. Velde, and G. Pinte, Geochemical comparison between minettes and kersantites from the Western European Hercynian Orogen: trace element and Pb-Sr-Nd isotope constraints on their origin, *Earth Planet. Sci. Lett.*, 87, 73-86, 1988.
- Wilson, M., Thermal evolution of the Central Atlantic passive margins: continental break-up above a Mesozoic superplume, *J. Geol. Soc. London*, 154, 491-495, 1997.
- Zangana, N.A., H. Downes, M.F. Thirlwall, and E. Hegner, Relationship between deformation, equilibration temperatures, REE and radiogenic isotopes in mantle xenoliths (Ray Pic, Massif Central, France): an example of plume-lithosphere interaction?, *Contr. Min. Pet.*, 127, 187-203, 1997.
- Zindler, A., and S. Hart, Chemical geodynamics, *An. Rev. of Earth. Plan. Sci.*, 14, 493-571, 1986.

Herve Bertrand, Ecole Normale Supérieure et UCBL, Laboratoire des Sciences de la Terre, UMR-CNRS 5570, Lyon, France; Herve.Bertrand@ens-lyon.fr

Mike Cosca, Institute of Mineralogy and Geochemistry, University of Lausanne, Switzerland; Mike.Cosca@imp.unil.ch

Denis Fontignie, Fred Jourdan, and Andrea Marzoli Section de Sciences de la Terre; Université de Genève, Switzerland; Jourdan6@etu.unige.ch; Andrea.Marzoli@terre.unige.ch; Denis.Fontignie@terre.unige.ch